Electronic Supplementary Material (ESI) for Journal of Materials Chemistry A.

A novel $LaCl_3$-based oxychloride solid-state electrolyte enables fast Li-ion transport and compatible with lithium metal

Xuxia Hao[a], Kai Chen[b]*, Min Jiang [b], Yanping Tang[b], Yuexin Liu[a], Kefeng Cai[a*]

[a]*Key Laboratory of Advanced Civil Engineering Materials of Tongji University, School of Materials Science & Engineering, Tongji University, 4800 Caoan Road, Shanghai 201804, China*

[b]*QingTao (Kunshan) Energy Development Co., Ltd., 215334, Suzhou, China*

* The corresponding author of this paper
Email: chenkai_qingtao@163.com
kfcai@tongji.edu.cn

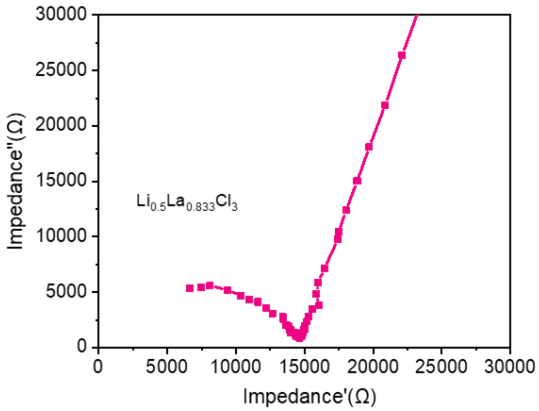

Fig. S1 Nyquist plots of $Li_{0.5}La_{0.833}Cl_3$.

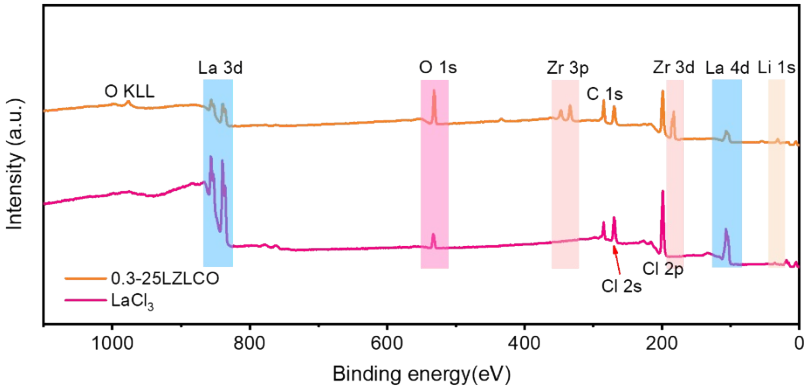

Fig. S2 The full spectrum of the $LaCl_3$ and 0.3-25LZLCO.

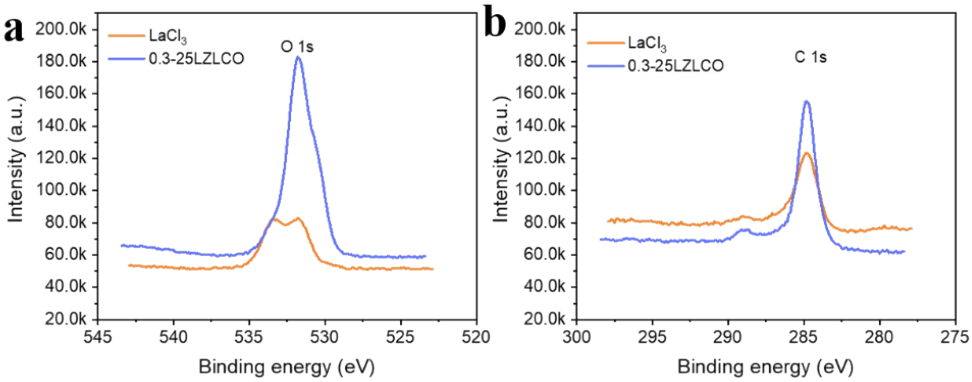

Fig. S3 a. O 1s and **b.** C1s XPS spectra of $LaCl_3$ and 0.3-25LZLCO.

During the XPS test, the O and C peaks usually appear due to the air pollution of the sample

surface. Based on the consistent testing process, the high-resolution spectrum of O 1s and C 1s peaks in $LaCl_3$ and 0.3-25LZLCO are shown in Fig. S3. The O 1s peak of LZLCO is considerably more intense than that for $LaCl_3$, with an amplitude that significantly exceeds the C 1s peaks. The results indicate that the potential experimental interference is negligible, and the increased intensity of the O 1s peak in the LZLCO spectrum may confirm the successful incorporation of oxygen into the $LaCl_3$ lattice.

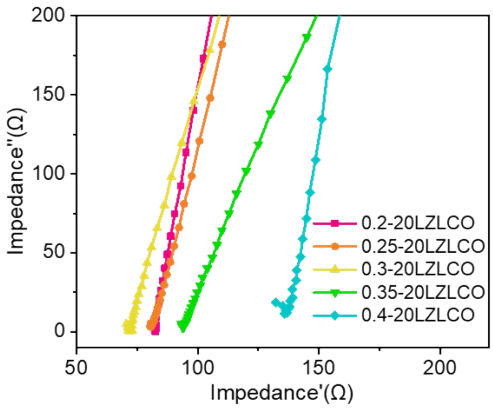

Fig. S4 Nyquist spectra of the x-20LZLCO (x = 0.2-0.4).

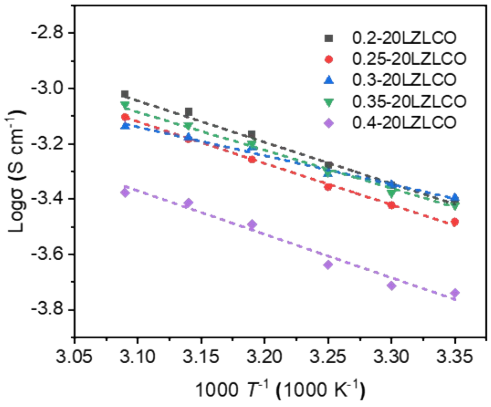

Fig. S5 Arrhenius plots of the x-20LZLCO (x=0.2-0.4).

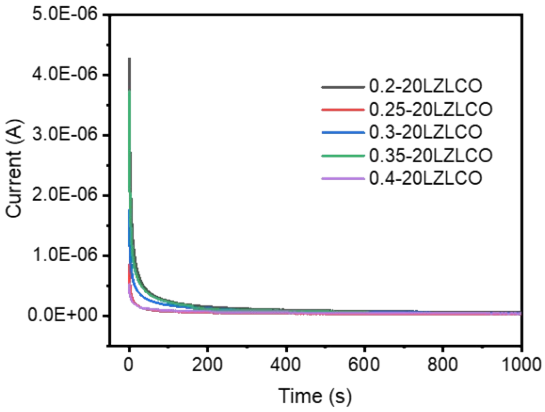

Fig. S6 Direct current polarization curve of the x-20LZLCO at 1 V.

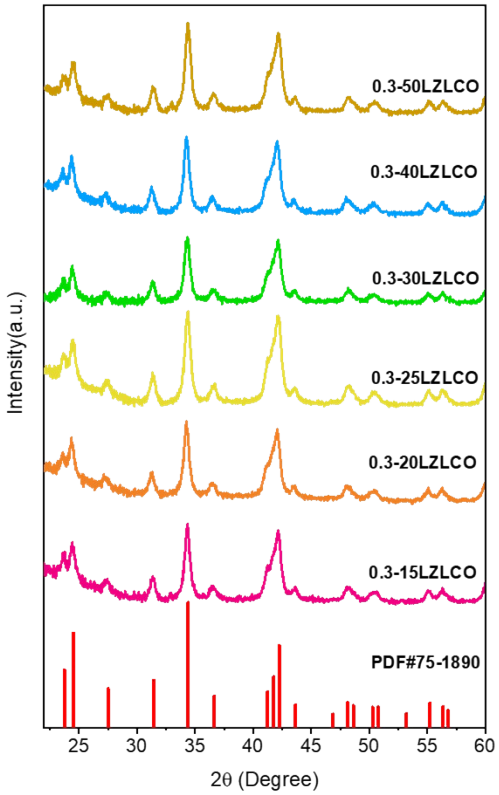

Fig. S7 XRD patterns of the 0.3-tLZLCO (t = 15-50 h).

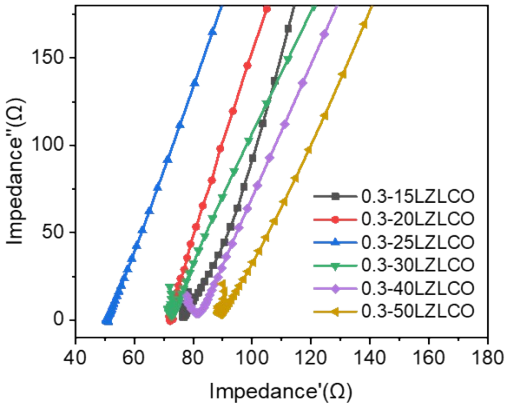

Fig. S8 Nyquist spectra of the 0.3-tLZLCO (t = 15-50 h).

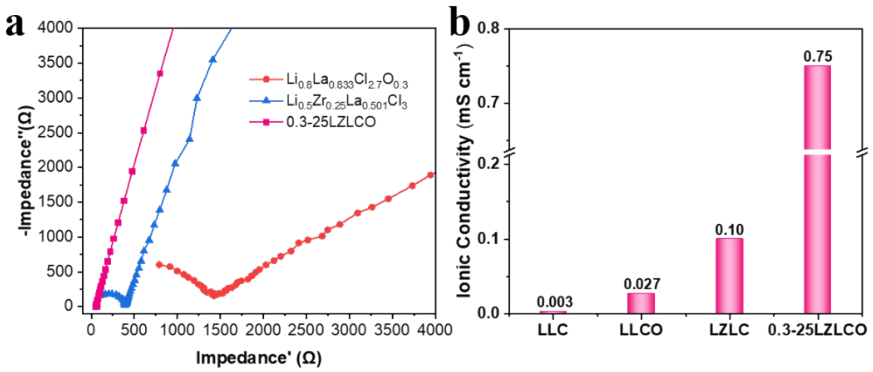

Fig. S9 a. Nyquist plots of $Li_{0.8}La_{0.833}Cl_{2.7}O_{0.3}$ (LLCO), $Li_{0.5}Zr_{0.25}La_{0.5}Cl_3$ (LZLC) and 0.3-25LZLCO. **b.** Histogram of ionic conductivities of $Li_{0.5}La_{0.833}Cl_3$ (LLC), $Li_{0.8}La_{0.833}Cl_{2.7}O_{0.3}$ (LLCO), $Li_{0.5}Zr_{0.25}La_{0.5}Cl_3$ (LZLC) and 0.3-25LZLCO.

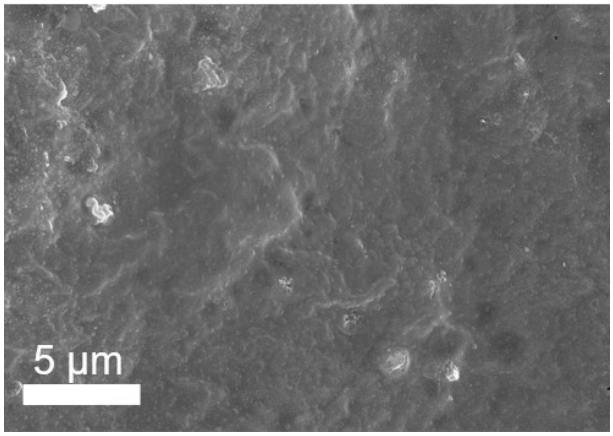

Fig. S10 Cross-sectional image of the 0.3-25LZLCO cold-pressed pellet at 375 MPa.

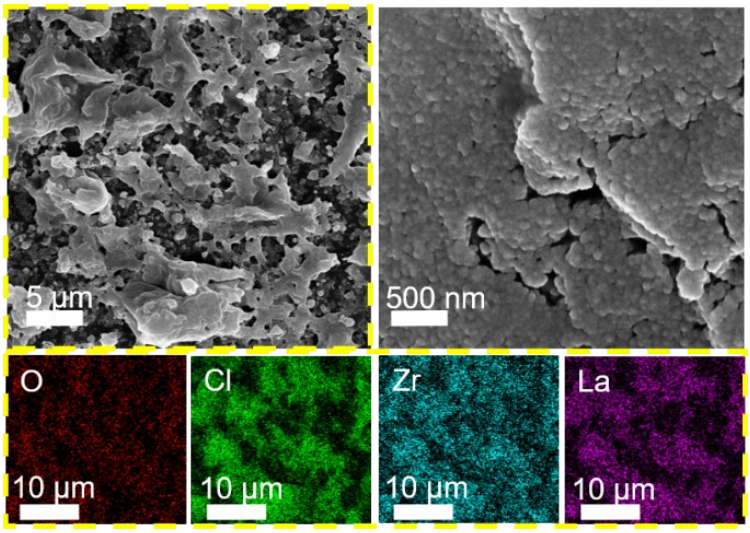

Fig. S11 SEM images of the 0.3-25LZLCO at different magnifications, and EDS mappings of O, Cl, Zr, La.

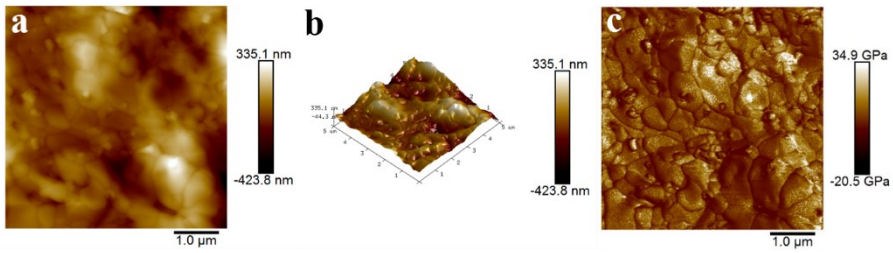

Fig. S12 a.) 2D image, **b.**) 3D image, and **c.**) Young's modulus of the 0.3-25LZLCO cold-pressed pellet by AFM test.

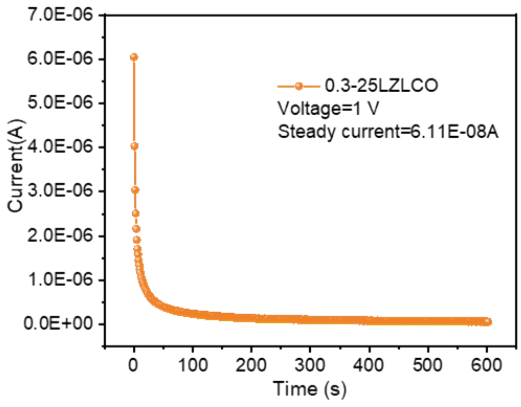

Fig. S13 Direct current polarization curve of the 0.3-25LZLCO at 1 V.

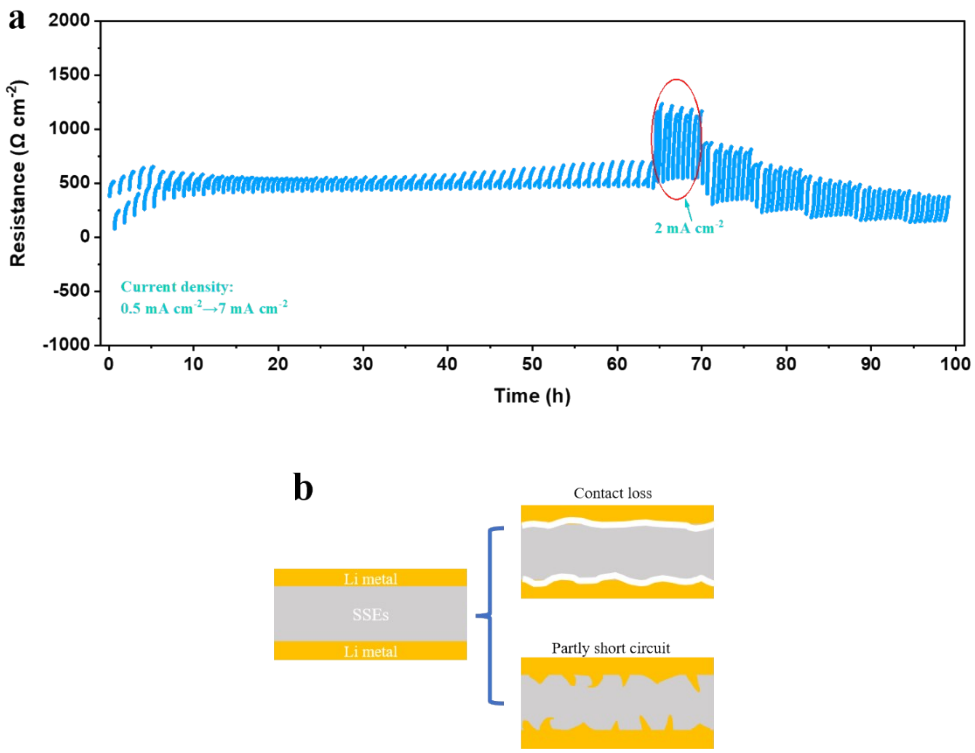

Fig. S14 a. The resistance of Li/0.3-25LZLCO/Li symmetry cell over time during the CCD test. **b.** Two types of interface failure of Li symmetry cell during the CCD test.

Further, we have constructed a resistance versus time curve (Fig. S15a) according to the CCD results of 0.3-25LZLCO. While the current density remains below 2 mA cm^{-2} with an increment rate of 0.1 mA cm^{-2}, the impedance remains relatively constant. However, as the current density ascends from 1 mA cm^{-2} to 2 mA cm^{-2} with a tenfold increase from the initial gradient, the interface impedance significantly increases. The increment can be associated with the contact loss of the interface between the lithium metal and electrolyte (shown in Fig. S15b), due to the volume expansion/shrinkage in the rapid lithium stripping of Li metal[1]. Upon further increasing the current density, the gradual decline in resistance can be ascribed to a minor partly short circuit at interface[2], as indicated in Fig. S15b. However, no hard or soft short circuit occurs, indicating that the 0.3-25LZLCO SSE can withstand the critical current density of 7 mA cm^{-2}.

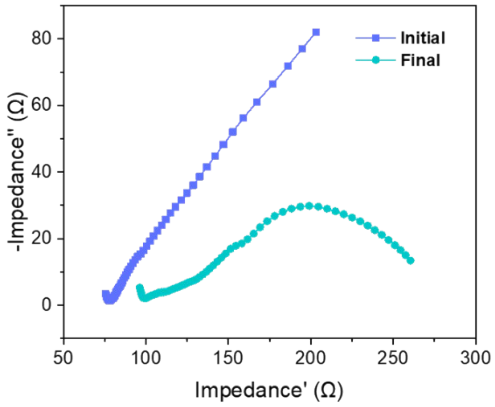

Fig. S15 Nyquist plots of ASSBs at the initial state and after 120 cycles at 0.2 C.

Table. S1 Electronic conductivities of xLZLCO with different O doping.

Samples with different O content	0.2-20LZLCO	0.25-20LZLCO	0.3-20LZLCO	0.35-20LZLCO	0.4-20LZLCO
Electronic conductivity	1.84	1.1	1.21	1.86	1.28

(10^{-9} S cm^{-1})	

Table. S2 Structural information of the 0.3-25LZLCO from the combined refinement of the XRD.Space group: $P6_3/m$

Atom	Wyckoff site	x/a	y/b	z/c	Occupancy	U_{iso} ($Å^2$)
La1	2c	1/3	2/3	1/4	0.6667	0.0336
Cl1	6h	0.09365	0.3891	3/4	0.7	0.0040
Li1	2b	0	0	0	1	0.18
Zr1	2c	1/3	2/3	1/4	0.33333	0.0336
O1	6h	0.0921	0.40543	3/4	0.3	0.004

References

1. P. Wang, W. Qu, W. L. Song, H. Chen, R. Chen and D. Fang, *Adv. Funct. Mater.*, 2019, **29**.
2. Y. Lu, C. Z. Zhao, H. Yuan, X. B. Cheng, J. Q. Huang and Q. Zhang, *Adv. Funct. Mater.*, 2021, **31**, 2009925.